Side Group-Mediated Mechanical Conductance Switching in Molecular Junctions

Ali Khalid Ismael[#], Kun Wang[#,] Andrea Vezzoli[#], Mohsin K. Al-Khaykanee, Harry E. Gallagher, Iain M. Grace, Colin J. Lambert[*], Bingqian Xu[*], Richard J. Nichols, and Simon J. Higgins[*]

#: these Authors contributed equally to this work.

*: Corresponding Authors

Dr. A. Vezzoli, Mr. H. E. Gallagher, Prof. Dr. R. J. Nichols, Prof. Dr. S. J. Higgins
Department of Chemistry, University of Liverpool, Crown Street, Liverpool L69 7ZD, U.K.
E-mail for Prof. Dr. S. J. Higgins: shiggins@liverpool.ac.uk
http://pcwww.liv.ac.uk/~nichols

Dr. K. Wang, Prof. Dr. B. Xu
College of Engineering & Department of Physics and Astronomy, University of Georgia, 220 Riverbend Road, Athens, GA 30602, U.S.A.
E-mail for Prof. Dr. B. Xu: bxu@engr.uga.edu
http://xulab.uga.edu

Dr. A. K. Ismael, Mr. M. K. Al-Khaykanee, Dr. I. M. Grace, Prof. Dr. C. J. Lambert
Department of Physics, Lancaster University, Lancaster LA1 4YB, U. K.
E-mail for Prof. Dr. C. J. Lambert: c.lambert@lancaster.ac.uk

Dr. A. K. Ismael
Department of Physics, College of Education for Pure Science, Tikrit University, Tikrit, Iraq

Mr. Mohsin K. Al-Khaykanee
Department of Physics, College of Science, University of Babylon, Iraq.

Abstract

A key target in molecular electronics has been molecules having switchable electrical properties. Switching between two electrical states has been demonstrated using such stimuli as light, electrochemical voltage, complexation and mechanical modulation. A classic example of the latter is the switching of 4,4'-bipyridine, leading to conductance modulation of ~1 order of magnitude. Here, we describe the use of side-group chemistry to control the properties of a single-molecule electromechanical switch, which can be cycled between two conductance states by repeated compression and elongation. While bulky alkyl substituents inhibit the switching behaviour, π-conjugated side-groups reinstate it. DFT calculations show that weak interactions between aryl moieties and the metallic electrodes are responsible for the observed phenomenon. This represents a significant expansion of the single-molecule electronics "tool-box" for the design of junctions with electromechanical properties.

Main Text

The ability to reliably cycle a metal-molecule-metal junction between two distinct conductive states is technologically important for the development of devices with transistor or switch properties, and could at the same time give valuable insights into the chemical and physical behaviour of isolated molecules at the nanoscale. So far, a variety of stimuli has been demonstrated to trigger a reversible change in the conductance state, the most studied being light and electrochemical potential. In these cases, the stimulus acts on the molecular backbone through which charge is transported, for instance by photoexcitation,[1] photoinduced E-Z isomerization[2] or cyclization[3–5] and electrochemical reduction or oxidation.[6–10] A conductance switch can be induced in a molecular device also through mechanical stimuli such as junction compression or elongation. In this case, the molecular component of the junction is left chemically unchanged, and the switching behaviour depends on the properties of the contacts and the molecule-metal interface. A classic example of this phenomenon is the switching of pyridyl-terminated molecular wires (such as 4,4'-bipyridine **1**) sandwiched between Au contacts, with a conductance modulation of ~1 order of magnitude upon junction compression-elongation.[11] In this case, the switching properties are due to the nature of the pyridyl-Au contact, which allows multiple coordination geometries. It is general consensus that junctions are in a "low conductance" state when the Au-N bond is perpendicular to the conducting π-system, and in a high conductance state when the junction is tilted, with the pyridyl ring lying co-facially on the metallic contact. Conductance changes upon mechanical modulation have also been observed in methyl-thioether terminated oligosilanes, where the behaviour is due to the stereoelectronic properties of the contacts and the orientation of the metallic lead with respect to the molecular backbone.[12] However, it has not been established how chemical design and substitution can be used to control such mechanically actuated molecular switches. In this submission, we studied the structural and chemical features necessary to control the reversible switching properties of a single molecule junction, based on functionalised biaryl compounds.

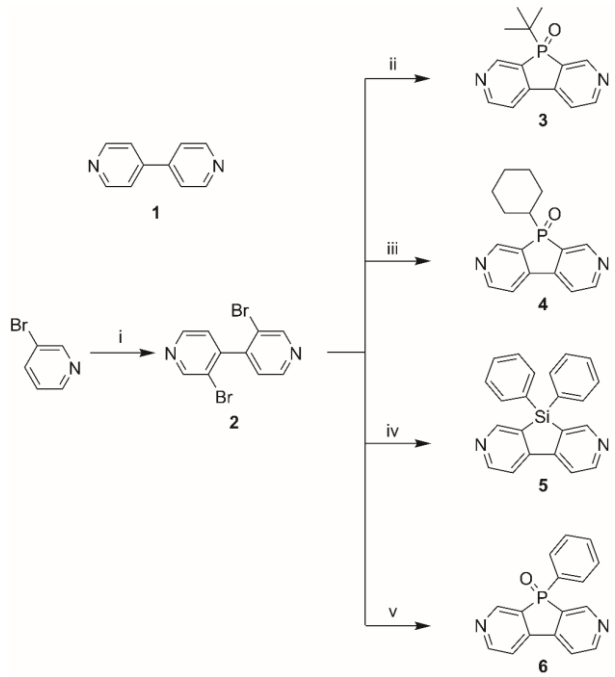

Figure 1: Structure of 4,4'-bipyridine **1** and synthetic pathway to compounds **2**-**6.** i) LDA (1 h, -94 ºC, THF), $CuCl_2$ (16 h, RT). ii) ^{n}BuLi, (1 h, -78 ºC, THF), ^{t}BuPCl_2 (15 min, 40 ºC), followed by H_2O_2 (4 h, RT, CH_2Cl_2) iii) ^{n}BuLi, (1 h, -78 ºC, THF), CyPCl_2 (15 min, 40 ºC), followed by H_2O_2 (4 h, RT, CH_2Cl_2). iv) ^{n}BuLi, (1 h, -78 ºC, THF), Ph_2SiCl_2 (16 h, RT). v) ^{n}BuLi, (1 h, -78 ºC, THF), PhPCl_2 (15 min, 40 ºC), followed by H_2O_2 (4 h, RT, CH_2Cl_2).

The substituted dipyridyls **2-6** were synthesised as described in Figure 1,[13,14] and the Scanning Tunnelling Microscopy - Break Junction (*STM-BJ*) technique[15] was used in this study to fabricate single-molecule junctions and to characterise their electrical behaviour. In brief, junctions are formed by repeatedly driving a gold tip into and out of contact with a gold substrate, in the presence of molecules with appropriate gold-binding end-group (adsorbed on the substrate). The current *I* is recorded during the withdrawal process, under a constant bias *V* of 300 mV, and transport through molecular bridges results in plateaux in the traces (examples in inset of Figure 2b). The process is repeated thousands of times and the results are compiled in histograms, where the plateaux in individual current-displacement traces result in peaks in the histograms that represent the distribution of conductance *G* values.

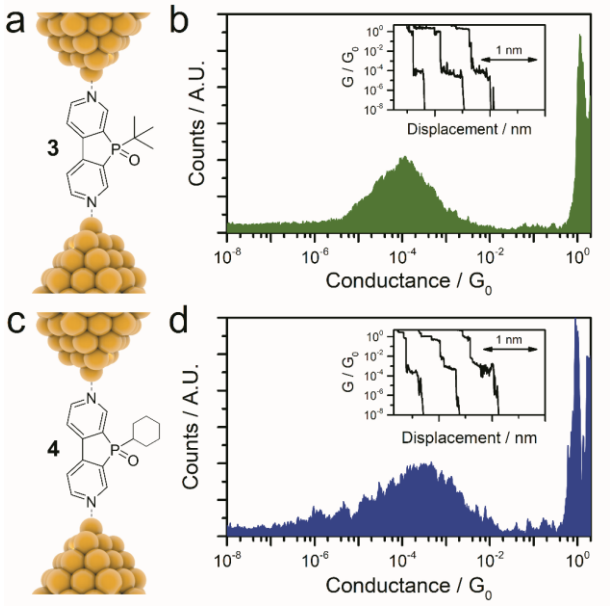

Figure 2: Structure of **3** (a) and **4** (c) in the Au-Au junction. Conductance histogram of **3** (b) and **4** (d), with example current-displacement traces as inset. Histograms compiled from >2000 current traces, at 20 nm s^{-1} withdrawal speed, using a tip-substrate bias of 300 mV. Conductance *G* is calculated using Ohm's law ($G = I / V$) and is given in units of the quantum of conductance $G_0 \approx 77.48$ μS.

The phosphoryl-bridged compounds **3** and **4** both produced quite broad conductance histograms although with no obvious signature of bistable conductance (Figure 2), in contrast with the clear double peak observed for **1**[16] and other pyridyl-terminated molecular wires.[17] The peak conductance values for **3** and **4** are lower than for unsubstituted **1**, with a most probable value of 2×10^{-4} G_0 for **3** and 3.5×10^{-4} G_0 for **4**. Although it may be tempting to suggest that there is non-switching behaviour, arising from rotational constraint of the two pyridyl rings with the molecule being unable to adopt one of the two possible geometries at the electrode contacts, the one-dimensional histograms are clearly very broad. Interestingly, although 3,3'-dibromo-4,4'-bipyridine **2** is also rotationally constrained (in this case, the dibromo substituents enforce orthogonality and make the coplanar geometry too high in energy), it nevertheless does show two clear peaks in the conductance histogram (details in the SI, Figure S1), and the values are consistent with the mechanism suggested by Quek et al.[11] To better understand the observed phenomena, we performed piezo-modulation experiments.[18–20] Here, the junction was first closed to achieve a conductance of several G_0, the tip was abruptly stretched ~1 (± 0.1) nm (d_s) to create a nanogap that could accommodate the dipyridyl molecule, and the size of this nanogap was then modulated by 0.2 nm (d_m) 4 times in 30 ms (modulation frequency of 135 Hz). The modulation value of 0.2 nm was chosen because it proved optimal to promote the switching between the high and low conductance states of 4,4'-bipyridine **1** (more details in the SI).[11] After this modulation, the junction

was stretched a further 1 nm, and hence broken. Example conductance traces along with their corresponding piezo-transducer (PZT) movement signal are shown in Figure 3.

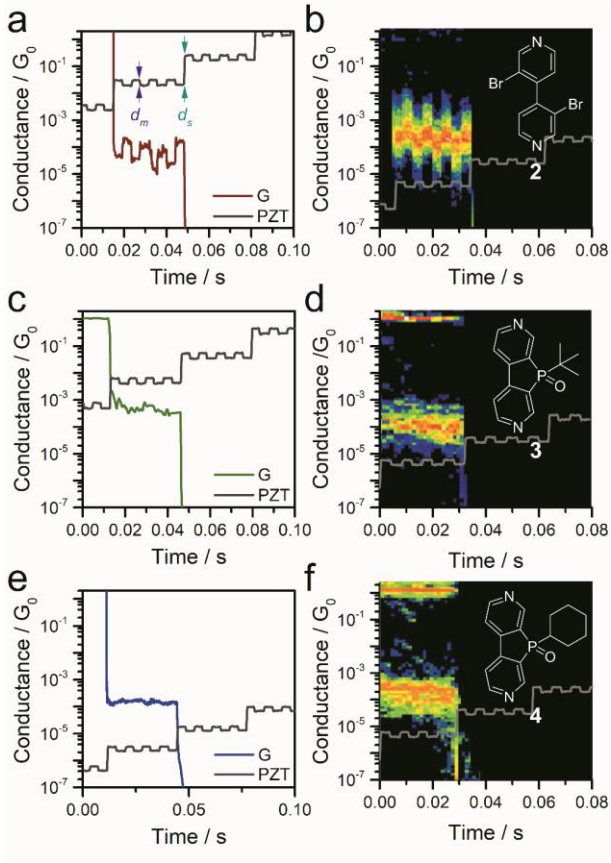

Figure 3: Example conductance vs time trace under piezo modulation for compounds **2** (a), **3** (c) and **4** (e), with piezo signal superimposed as grey line. Modulation 2d density maps for compounds **2** (b), **3** (d) and **4** (f). Structure and piezo signal are superimposed on the 2d maps for clarity.

Compound **2** behaved similarly to 4,4'-bipyridine **1**, with a switching of about 1 order of magnitude upon piezo modulation (Figure 3b). This phenomenon has been ascribed to different geometries at the Au-N interface adopted by the molecule upon junction compression and stretching.[11] In contrast, **3** and **4** showed no conductance switching at all, and the modulation only resulted in increased noise (Figure 3d and 3f, respectively). We reasoned that the presence of bulky alkyl side-groups effectively prevent the molecule from adopting the "high" conductance geometry suggested by Quek et al[11] by simple steric hindrance. It is, therefore, an effective way to shut down the mechanically triggered conductance switching of such molecular junctions.

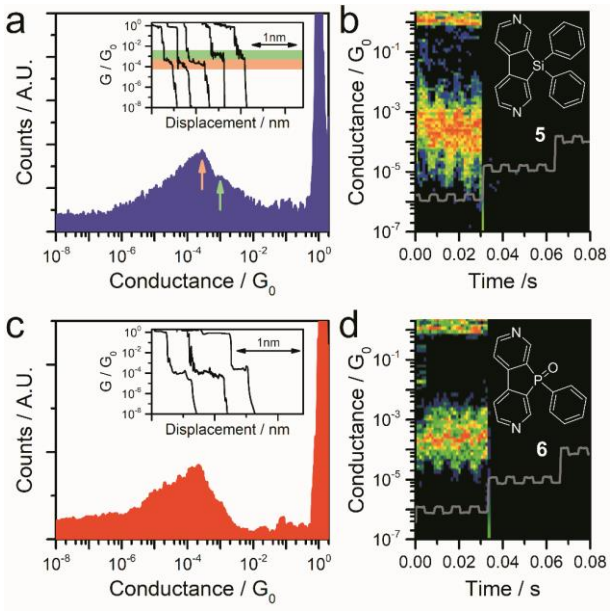

Figure 4: Conductance histogram (a) with example traces as inset, and modulation 2d density map (b) for compound **5**. Conductance histogram (c) with example traces as inset, and modulation 2d density map (d) for compound **6**. Experiments performed at 300 mV tip-substrate bias. Piezo signal as grey line and the molecular are superimposed on the 2d maps for clarity.

To further investigate this phenomenon, we turned our attention to the Si-bridged dipyridyl **5**, with two orthogonal phenyl rings on the heteroatom. *STM-BJ* measurements on **5** resulted in a broad peak in its conductance histogram, with a maximum at 2×10^{-4} G_0 and a pronounced shoulder at 10^{-3} G_0 (Figure 4a). Interestingly, piezo-modulation experiments on **5** showed the signature of cycling through the two conductance states instead of shutting down the conductance switching as in the case of compound **4** (example conductance traces in Figure S2 of the SI). Metal/molecule/metal junctions with phenyl rings acting as contacts (*e.g.* through η^2 coupling) have been reported in the literature, for instance in cyclophanes[21], C_{60},[22] and organometallic molecular wires.[23] We therefore hypothesised that the switching mechanism proposed by Quek *et al.*[11] is disabled in **3** and **4** due to the steric bulk of the alkyl substituents, but interactions of a side π-system with the metallic lead reinstate the binary conductance behaviour. To further test this hypothesis and determine whether it is the Si bridge or the side-group responsible for the switching properties, we prepared **6**, which has a phenyl moiety on a phosphoryl bridge. In Figure 4d, the piezo-modulation measurements on **6** revealed clear conductance switching (example conductance traces in Figure S2 of the SI). In the case of **6** (phosphoryl bridge), the average ratio between the two conductance states is only ≈ 2, increasing to ≈ 5 in **5** (Si bridge). Therefore, *STM-BJ* measurements confirmed that it is the aryl substituent that reinstates conductance switching, although the bridging heteroatom identity modulates its magnitude. As further evidence for the

proposed mechanism, we noted that the piezo-modulation density maps for compounds **5** (Figure 4b) and **6** (Figure 4d) show noisier switching than **2** (Figure 3b), consistent with the high mobility of the phenyl side-substituent responsible for the increase in conductance. It was also found that the switching behaviour is retained at a higher modulation frequency (400 Hz, see Supporting Information, Figure S4). To validate the proposed switching mechanism, we performed DFT quantum transport calculations, exploring both the Au-pyridyl contact geometry and the binding characteristics of the side group on the metalloid bridge. As described in the SI, a variety of different junction geometries were explored (for more details, see figures S6 to S14), to assess the most likely configuration of the molecular bridge and the molecule-electrode coupling strength. The geometry which showed the higher binding energy (see figure S6) in the compressed junction and better explained the experimental results is the one where the dipyridyl unit lies tilted between the two leads, with a N terminus contacted to an under-coordinated Au atom and the other end in a co-facial arrangement with the Au electrode. Results of DFT calculations on **4** and **5** are presented in Figure 5. In the relaxed junction, the molecular bridge lies parallel to the electrode axis, and transport is LUMO-dominated, with a sharp resonance near E_F. Upon junction compression, the molecular bridge tilts in the junctions to reach the described geometry where the pyridyl ring lies co-facially to the electrode. While it has previously been shown that such arrangement leads to an increase in conductance, in the case of **4** there is little difference in the transmission curves *T(E)* for the relaxed geometry A and the compressed B. The bulky side-group of **4** causes the Au-N bond to stretch to ~ 0.3 nm, reducing the binding energy and the coupling to the electrode. The shorter charge transport pathway is therefore countered by the weak coupling, resulting in no broadening of the resonances in the *T(E)* curves and negligible change in the conductance value.

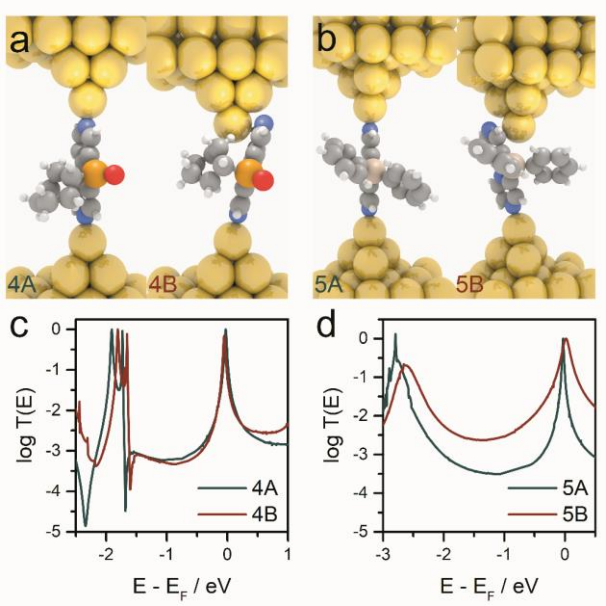

Figure 5: DFT-optimised geometries for compound **4** (a) and **5** (b), in the relaxed (A) and compressed (B) geometry. Relative transmission curves in each geometry for **4** (c) and **5** (d).

T(E) for compound **5** (Figure 5d) shows a different behaviour, with a broadening of molecular resonances resulting a clear increase in the off-resonant transmission values upon junction compression, that can be ascribed to an increase in the molecule-lead coupling strength. The binding geometry at the co-facial end does not change from **4** (Figure 5a and 5b), and consequently the resonance broadening arises from interactions between the π-system of the phenyl side-groups and the Au electrode, which increase the overall coupling. Performing the same calculations on **3** and **6** resulted in a similar predicted behaviour (details in the SI). We note that the introduced transport mechanism represents the first example of conductance switching mediated by apparently innocuous substituents orthogonal to the conductance path, which have no continuous σ-bond with the junction leads. Furthermore, our study highlights the need for a more thorough characterisation of single-molecule junctions beyond the traditional crash-withdraw *STM-BJ* technique, as many subtle but important effect can be hidden in the broad distribution of conductance values routinely observed in one-dimensional histograms.

In conclusion, we presented the synthesis and single-molecule conductance measurements of a family of planarized 4,4'-dipyridyls, with the two rings bridged in 3 and 3' position by a heteroatom. The resulting planarization (with formation of a 5-membered ring) and the presence of bulky orthogonal substituents effectively switch off the mechanically controlled binary conductance switching of 4,4'-dipyridyl **1**,[11] by reducing the molecule-lead coupling strength in the high-conductance geometry. The phenomenon can be reinstated by introducing aryl orthogonal substituents, which cause a broadening of

the transport resonance by interacting with the Au leads. The extent of switching depends on the bridging heteroatom (conductance change of P-bridged **6** = 1×10^{-4} G_0 and Si-bridged **5** = 8×10^{-4} G_0), showing the subtle effect of entities outside of the main conjugation path on the behaviour of single-molecule junctions. We envisage that the mechanism of conductance switching demonstrated here may stimulate the synthesis and testing of other related molecules.

Experimental Section

Synthetic procedures for the compounds used in this study, technical details on the STM measurements, further information and parameters for the theoretical calculations, and additional experimental and computational results can be found in the Supporting Information.

Data Availability

NMR spectra for compounds 2 - 6 are available in the data catalogue in Liverpool at: https://datacat.liverpool.ac.uk/id/eprint/405

Acknowledgements

This work was supported by UK EPSRC (grants EP/H035184/1, EP/M005046/1, EP/N017188/1 and EP/M014452/1), US NSF (grants ECCS 1231967 and ECCS 1609788), European Commission (project 606728 of FP7 ITN "MOLESCO") and the Iraqi Ministry of Higher Education (SL-20). A.K.I. acknowledges financial support from Tikrit University (Iraq), and M. K. A. acknowledges financial support from Babylon University (Iraq).

References

[1] S. Battacharyya, A. Kibel, G. Kodis, P. a Liddell, M. Gervaldo, D. Gust, S. Lindsay, *Nano Lett.* **2011**, *11*, 2709–14.

[2] S. Martin, W. Haiss, S. J. Higgins, R. J. Nichols, *Nano Lett.* **2010**, *10*, 2019–2023.

[3] N. Darwish, A. C. Aragonès, T. Darwish, S. Ciampi, I. Díez-Pérez, *Nano Lett.* **2014**, *14*, 7064–7070.

[4] D. Roldan, V. Kaliginedi, S. Cobo, V. Kolivoska, C. Bucher, W. Hong, G. Royal, T. Wandlowski, *J. Am. Chem. Soc.* **2013**, *135*, 5974–5977.

[5] C. Jia, A. Migliore, N. Xin, S. Huang, J. Wang, Q. Yang, S. Wang, H. Chen, D. Wang, B. Feng, et al., *Science* **2016**, *352*, 1443–1445.

[6] W. Haiss, H. van Zalinge, S. J. Higgins, D. Bethell, H. Höbenreich, D. J. Schiffrin, R. J. Nichols, *J. Am. Chem. Soc.* **2003**, *125*, 15294–5.

[7] Z. Li, I. Pobelov, B. Han, T. Wandlowski, A. Błaszczyk, M. Mayor, *Nanotechnology* **2007**, *18*, 44018.

[8] B. Q. Xu, X. L. Li, X. Y. Xiao, H. Sakaguchi, N. J. Tao, *Nano Lett.* **2005**, *5*, 1491–5.

[9] T. C. Ting, L. Y. Hsu, M. J. Huang, E. C. Horng, H. C. Lu, C. H. Hsu, C. H. Jiang, B. Y. Jin, S. M. Peng, C. H. Chen, *Angew. Chemie - Int. Ed.* **2015**, *54*, 15734–15738.

[10] Y. Li, M. Baghernejad, A.-G. G. Qusiy, D. Zsolt Manrique, G. Zhang, J. Hamill, Y. Fu, P. Broekmann, W. Hong, T. Wandlowski, et al., *Angew. Chemie - Int. Ed.* **2015**, *54*, 13586–13589.

[11] S. Y. Quek, M. Kamenetska, M. L. Steigerwald, H. J. Choi, S. G. Louie, M. S. Hybertsen, J. B. Neaton, L. Venkataraman, *Nat. Nanotechnol.* **2009**, *4*, 230–234.

[12] T. a. Su, H. Li, M. L. Steigerwald, L. Venkataraman, C. Nuckolls, *Nat. Chem.* **2015**, *7*, 1–6.

[13] S. Durben, T. Baumgartner, *Angew. Chem. Int. Ed. Engl.* **2011**, *50*, 7948–52.

[14] J. Ohshita, K. Murakami, D. Tanaka, Y. Ooyama, T. Mizumo, N. Kobayashi, H. Higashimura, T. Nakanishi, Y. Hasegawa, *Organometallics* **2014**, *33*, 517–521.

[15] B. Xu, N. Tao, *Science* **2003**, *301*, 1221–1223.

[16] T. Kim, P. Darancet, J. R. Widawsky, M. Kotiuga, S. Y. Quek, J. B. Neaton, L. Venkataraman, *Nano Lett.* **2014**, *14*, 794–798.

[17] P. Moreno-García, M. Gulcur, D. Z. Manrique, T. Pope, W. Hong, V. Kaliginedi, C. Huang, A. S. Batsanov, M. R. Bryce, C. Lambert, et al., *J. Am. Chem. Soc.* **2013**, *135*, 12228–40.

[18] K. Wang, J. M. Hamill, J. Zhou, B. Q. Xu, *J. Am. Chem. Soc.* **2014**, *136*, 17406–9.

[19] K. Wang, B. Q. Xu, *Phys. Chem. Chem. Phys.* **2016**, *18*, 9569–9576.

[20] K. Wang, J. Hamill, J. Zhou, C. Guo, B. Q. Xu, *Faraday Discuss.* **2014**, *174*, 91–104.

[21] S. T. Schneebeli, M. Kamenetska, Z. Cheng, R. Skouta, R. A. Friesner, L. Venkataraman, R. Breslow, *J. Chem. Soc. Chem. Commun.* **2011**, *133*, 2136–2139.

[22] H. Park, J. Park, A. A. K. L. Lim, E. E. H. Anderson, A. P. A. Alivisatos, P. L. P. McEuen, *Nature* **2000**, *407*, 57–60.

[23] O. A. Al-Owaedi, S. Bock, D. C. Milan, M.-C. Oerthel, M. S. Inkpen, D. S. Yufit, A. N. Sobolev, N. J. Long, T. Albrecht, S. J. Higgins, et al., *Nanoscale* **2017**, DOI 10.1039/C7NR01829K.

Table of Content

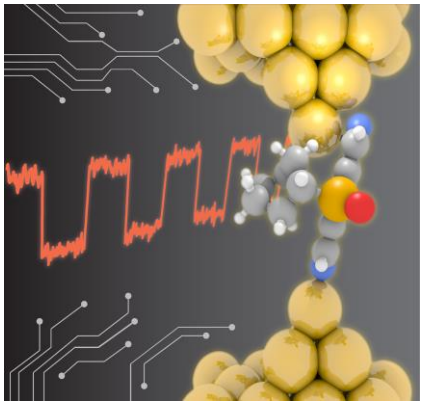

Designing molecular switches: The criteria for the development of single-molecule electromechanical switches are presented in the manuscript. Conjugate moieties that provide additional coupling to the metallic electrodes of a single-molecule junction increase the electron transmission efficient and promote charge transport. The junction can therefore be cycled between two conductance states by acting on the separation between the two electrodes, and chemical design can be used to tune the extent of switching.

Keywords:

- Molecular Electronics
- Electron Transport
- Nanotechnology
- Scanning Probe Microscopy
- Density Functional Calculations